Multisensory learning binds modality-specific neurons into a cross-modal memory engram

Abbreviated title: Multisensory learning expands a memory engram

Zeynep Okray[1,2], Pedro F. Jacob[1,2], Ciara Stern[1], Kieran Desmond[1], Nils Otto[1], Paola Vargas-Gutierrez[1], and Scott Waddell[1,*]

[1]Centre for Neural Circuits & Behaviour, University of Oxford, Oxford, OX1 3TA, United Kingdom

[2]These authors contributed equally to this work

*Corresponding author and Lead contact: Scott Waddell (scott.waddell@cncb.ox.ac.uk)

Conflict of Interest: The authors declare no competing financial interests.

Abstract

Associating multiple sensory cues with objects and experience is a fundamental brain process that improves object recognition and memory performance. However, neural mechanisms that bind sensory features during learning and augment memory expression are unknown. Here we demonstrate multisensory appetitive and aversive memory in *Drosophila*. Combining colors and odors improved memory performance, even when each sensory modality was tested alone. Temporal control of neuronal function revealed visually-selective mushroom body Kenyon Cells (KCs) to be required for both enhancement of visual and olfactory memory after multisensory training. Voltage imaging in head-fixed flies showed that multisensory learning binds activity between streams of modality-specific KCs, so that unimodal sensory input generates a multimodal neuronal response. Binding occurs between regions of the olfactory and visual KC axons, which receive valence-relevant dopaminergic reinforcement, and is propagated downstream. Dopamine locally releases GABA-ergic inhibition to permit specific microcircuits within KC-spanning serotonergic neurons to function as an excitatory bridge between the previously 'modality-selective' KC streams. Cross-modal binding thereby expands the olfactory memory engram by recruiting visual path KCs to become odor responsive. This broadening of the engram improves memory performance after multisensory learning and permits a single sensory feature to retrieve the memory of the multimodal experience.

Life is a rich multisensory experience for most animals. As a result, nervous systems have evolved to integrate sensory information into multisensory representations of objects, scenes and events to most effectively guide behavior[1]. It is widely appreciated that multisensory learning can improve memory performance, from children in the classroom to rodents and insects in controlled experiments in the laboratory[2–4]. Moreover, an apparently universal and unexplained feature of multisensory learning is that it improves subsequent memory performance even for the separate unisensory components[3]. Cells that respond to multiple sensory cues have been identified in different places in the human/mammalian brain and the proportions/numbers have been reported to change after multisensory learning[1,5–7]. However, it is unclear whether and how multisensory learning converts neurons from being modality selective to being multimodal, and how memory performance could be supported by such a process.

In *Drosophila*, unique populations of mushroom body (MB) Kenyon Cells (KCs) receive predominant and anatomically segregated dendritic input from olfactory or visual projection neurons (as well as local visual interneurons) and their axons project as parallel streams into the MB lobes. In the lobes, successive compartments of each KC's axonal arbor are intersected by the presynapses of dopaminergic neurons (DANs) that convey the reinforcing effects of appetitive or aversive stimuli[8,9]. Reinforcing dopamine depresses synapses between active KCs and the compartment-restricted dendrites of downstream mushroom body output neurons (MBONs) to code valence-specific memories[10,11].

To study multisensory learning and memory in *Drosophila* we adapted the olfactory T-maze[12] so that odors and colors can be presented together (Fig. 1a). Food-deprived flies were trained by presenting them with an color and/or odor (conditioned stimulus minus, CS−), followed by another odor and/or color (conditioned stimulus plus, CS+) paired with sugar reward (Fig. 1a-b). When trained and tested with only colors [visual learning, V], flies did not show a significant learned preference for the previously sugar paired color (Fig. 1b-d; Extended Data Fig. 1a). However, combining colors with odors [congruent protocol, C] produced a robust and long-lasting memory, which was significantly enhanced over that formed by training with only odor cues [olfactory learning, O] (Fig. 1b-d, and Extended Data Fig. 1a-b). If the odor and color combinations were swapped between training and testing [incongruent protocol, I] (Fig. 1b-d; Extended Data Fig. 1a-b), no memory enhancement was observed. Furthermore, a marked memory enhancement was not apparent if the same color was presented with the CS- and CS+ odors during training and testing (Extended Data Fig. 1c). The memory enhancing effect of multisensory learning therefore requires a learned relationship between specific odor and color combinations. Interestingly, for memory measured 6 h after training, the incongruent

protocol revealed significantly decreased performance compared to that following odor only training (Fig. 1d), suggesting that flies are conflicted when faced with a switch of the odor-color contingency between training and testing.

To further investigate the nature of multimodal memory enhancement, we restricted the presentation of the multisensory cues to either training or testing. Multisensory training improved memory retrieval even when each sensory modality was presented alone during testing [olfactory retrieval, OR; visual retrieval, VR] (Fig. 1e,f). In contrast, presenting multisensory stimuli only during the memory test, but not during training, did not facilitate performance [multisensory retrieval, MSR] (Extended Data Fig. 1d). Moreover, the greatest improvement in memory performance was observed when multisensory stimuli were used both during training and testing (Extended Data Fig. 1e). Therefore, multisensory training enhances memory performance for the individual odor and color memory components, and congruence of odor and color information between training and testing further enhances performance. Although our experiments and those of others[13,14] imply that flies can distinguish green and blue colors, we do not at this point discount a contribution of hue and luminance.

The dendrites of the numerically larger populations of olfactory KCs within the αβ, α′β′ and γ lobes occupy the main calyces of the MB, whereas the relatively small populations of αβ posterior ($\alpha\beta_p$) and γ dorsal (γd) KCs receive predominantly visual information via their dendrites in the accessory calyces[9]. The γd KCs have previously been implicated in color learning[13,15]. We tested the role of visual γd and $\alpha\beta_p$ KCs in multisensory learning and memory, using cell-specific expression of a UAS-*Shibire*^{ts1} (*Shi*^{ts1}) transgene which encodes a dominant temperature-sensitive dynamin[16]. At temperatures >30 ˚C, *Shi*^{ts1} blocks membrane recycling and thus impairs synaptic transmission while function can be restored by returning flies to <29˚C. Blocking output from γd and $\alpha\beta_p$ KCs during testing at 6h abolished the visual enhancement of performance in the congruent protocol, and removed the interference effect in the incongruent protocol in both instances memory performance was similar to that of flies tested with odors alone (Fig. 2a-d, Extended Data Fig. 2a-f). These results are consistent with activity in γd and $\alpha\beta_p$ KCs representing the visual component of multisensory memory (see also, Extended Data Fig. 2g-h). Surprisingly, blocking transmission from γd KCs (but not $\alpha\beta_p$ KCs) during testing also impaired performance for odor-only memory retrieval in multisensory trained flies (Fig. 2e-f), despite having no effect on memory retrieval in flies trained with only odors (Extended Data Fig. 2a,d). This unexpected result led us to hypothesize that multisensory learning might expand the KC representation of odors to include ‘visual’ γd KCs.

To directly test for learned odor-evoked responses in γd KCs after multisensory training, we expressed the voltage sensor UAS-ASAP2f[17] in γd KCs and performed two-photon functional imaging (Fig. 3a-d,g-j). We trained flies in the T-maze using a multisensory (color+odor), unisensory (odor), or unpaired protocol (where sugar was presented 2 min after color+odor). 6 h after training, flies were imaged for their CS− and CS+ odor responses. Recordings of γd KC axons were made in the terminal γ5 compartment of the MB horizontal lobe, since key sugar rewarding dopaminergic neurons (DANs) drive learning-relevant presynaptic depression of KC-MBON synapses in the γ4 and γ5 compartments[18–20]. For comparison we also imaged γd KC responses in the more proximal γ1 compartment, which houses the presynaptic field of DANs that provide aversive teaching signals[21–26]. Odor presentation was previously shown to evoke slow inhibitory responses in γd[13] and $\alpha\beta_p$ KCs[27] of naïve flies. Consistent with these findings, presentation of the CS- odor evoked hyperpolarisation of γd KCs in both the γ1 and γ5 compartments, regardless of the training protocol (Fig. 3a-d and Extended Data Fig. 3a-b; light purple trace). However, after multisensory training the CS+ odor produced a significant depolarization of γd KC axons in the γ5 compartment (Fig. 3a, dark purple trace). CS+ responses in γ1 appeared to be less inhibited than those of the CS- (Fig. 3b, although the responses were statistically indistinguishable) perhaps as a result of the hunger-state dependent control of the γ1pedc DAN[28–30]. Importantly, the multisensory training driven sign reversal of the γd KC odor response in γ5 did not occur following unisensory odor only (Fig. 3c; dark purple trace trace) or unpaired training (Extended Data Fig. 3a-b; dark purple trace). In these cases both the CS+ and CS- odors evoked hyperpolarization of γd KCs in the γ1 and γ5 compartments. These results indicate that dopaminergic reward teaching signals broaden CS+ odor-evoked excitation within the γ KC ensemble by recruiting the γ5 segments of γd KC axons to become odor activated. This larger odor memory engram provides a mechanism for how odor memory performance is enhanced following multisensory training, and explains why odor memory retrieval in this context acquires a requirement for γd KC output (Fig. 3e).

If DANs direct the recruitment of γd axons to become odor activated, a learning event that engages DANs innervating a distinct compartment should confer odor-responsiveness onto a different downstream segment of γd axons. Aversive memory formation requires dopamine release from neurons including the PPL1-γ1pedc DANs that innervate the most proximal γ lobe compartment - γ1[31]. We first confirmed that multisensory odor and color aversive (electric shock punishment) training produced a memory enhancement for both the combined and individual cues, similar to that observed after multisensory appetitive training (Fig. 3f, Extended Data Fig. 3c-h). We next used 2-photon imaging of the ASAP2f voltage sensor to test whether γd axons from γ1 onwards gained CS+ odor activation after multisensory aversive

learning. Presentation of the CS- odor evoked hyperpolarisation of γd KCs in both the γ1 and γ5 compartments, regardless of the training protocol (Fig. 3g-j and Extended Data Fig. 3 i-j; light purple trace). In contrast, exposure to the CS+ odor after multisensory aversive training produced brief excitation of γd KCs in the γ1 and γ5 compartments. Recordings of odor-evoked responses in γd KCs following appetitive and aversive multisensory learning are therefore consistent with the location of dopaminergic teaching signals determining the portion of γd axons that becomes activated by the CS+ odor. Whereas aversive learning makes all of the γd axon segments downstream of γ1 excitable by the CS+ odor (Fig. 3f), reward learning primarily alters the CS+ excitation within the terminal γ4 and γ5 segments (Fig. 3e).

An expansion of the CS+ odor representation into a particular segment of the γd axons after multisensory training might be expected to facilitate subsequent learning with the same odor, if the next dopamine teaching signal intersects the expanded KC representation. We tested this notion by sequentially training flies with either an aversive (dopamine in γ1) or appetitive (dopamine in γ4 and γ5) multisensory protocol followed by unisensory odor-reward or odor-punishment learning (Fig 3k-l), respectively. Prior multisensory aversive training significantly enhanced subsequent odor-reward learning (Fig. 3k). However, no performance enhancement was apparent if aversive odor learning followed multisensory appetitive learning (Fig. 3l). Therefore the multisensory training-dependent expansion of the CS+ odor representation can be included into the next CS+ odor memory engram if the appropriate γd axon segments have become CS+ odor-activated.

The anatomy of the MB network suggests two possible ways for odor responsiveness to be conferred to γd KC axons: via KC-KC synapses or neurons positioned to bridge the different KC streams. We queried the anatomical feasibility of these routes using the complete MB connectome of the adult female fly 'hemibrain' electron microscope (EM) volume[32,33]. Although most (562 of 590) γm KCs make synapses with γd KCs, the number and placement of these connections does not support every γd KC to receive γm input in every γ lobe compartment. In addition, KC-KC connections have also been reported to suppress activity in neighboring KCs[34]. We next studied the fine anatomy of the γ lobe innervation of the potentially excitatory serotonergic Dorsal Paired Medial (DPM) neuron in the hemibrain EM volume. DPM neurons send separate branches that densely innervate the vertical and horizontal lobes and distal peduncle of the MB, where they are both pre- and post-synaptic to the KCs[35–38]. Analyzing the ultrastructure of DPM neuron projections in the horizontal γ lobe revealed two branches within the γ1 compartment and other ventral and dorsal branches passing through the γ2 - γ5 compartments (Fig. 4a). The positions of DPM neuron synapses onto γd KCs follow the γd KC

axon bundle as it winds around the γ lobe from ventral in γ1 to dorsal in the γ5 compartment (Fig. 4a).

Annotating a dendrogram of DPM neuron neurites (Fig. 4b) with γ lobe compartment boundaries (based on DAN connectivity), synapses from γm KCs and those to γd KCs, showed that unique branches of the DPM neuron can provide compartment-specific microcircuit bridges between γm and γd KCs. DPM neurons can also bridge γd to γm KC connectivity (Extended Data Fig. 4g). The large GABAergic anterior paired lateral (APL)[37,39] neuron was found to make synapses along the DPM branches in the γ lobe (Fig. 4b and Extended Data Fig. 4h), suggesting DPM bridging can be regulated by inhibition. Importantly, the APL neuron receives many DAN inputs within each compartment and can therefore also be regulated with region specificity (Extended Data Fig. 4h), to potentially release specific DPM branches from APL inhibition.

We challenged this putative microcircuit bridge model by independently manipulating the APL and DPM neurons. Expression in APL neurons of the DopR2 dopamine receptor has been linked to aversive learning[40] and transciptional profiling suggests APL neurons also express the DopEcR receptor[41]. Both of these dopamine receptors are known to be inhibitory[42,43]. We therefore used *tub*P-GAL80^{ts} [44] to temporally-restrict transgenic RNAi in APL neurons to test for a role of these receptors in multisensory learning. Knocking down Dop2R in adult APL neurons abolished the multisensory enhancement of odor memory performance (Fig. 4c). A mild defect was also observed for odor memory following olfactory appetitive conditioning, however the difference was only significant to one of the controls (Fig. 4d). In contrast, DopEcR RNAi did not produce a defect in either experiment (Extended Data Fig. 4a-b). These results are consistent with reinforcing dopamine inhibiting APL neurons to allow the recruitment of γd KCs into the olfactory memory engram during multisensory learning.

We next tested for a role of the serotonergic DPM neurons using expression of UAS-*Shi*^{ts1}. Temporally restricting neurotransmission from DPM neurons either during the acquisition (Fig. 4e) or retrieval (Fig. 4f) phases significantly impaired the multisensory training enhancement of odor memory performance. These same manipulations had no effect on odor memory performance after unisensory olfactory learning (Extended Data Fig. 4e), consistent with prior work[45]. We propose that DPM neuron output is required for learning because it binds together simultaneously active KC streams, whereas DPM neuron output during memory retrieval provides the connection for odor-driven γm KCs to activate the relevant γd KCs. Serotonin (5-hydroxytryptamine, 5-HT) can exert excitatory effects through 5-HT2A and 5-HT7 type receptors[46]. We therefore used RNAi to knockdown these 5HT receptors in γd KCs and tested olfactory memory following multisensory training. Reducing 5-HT2A but not 5-HT7 or 5-HT2B

receptor expression impaired memory performance (Fig. 4g). Moreover, bath application of 5-HT evoked a clear excitatory response in γd KCs expressing ASAP2f in naïve flies (Fig. 4h-i). Taken with prior knowledge that learning specifically increases responsiveness of DPM neurons to the CS+ odor[36], these anatomical, genetic and physiological data lead us to conclude that reinforcer-evoked compartment specific dopamine releases APL-mediated inhibition which permits the formation of an odor-color specific DPM microcircuit bridge between the relevant γm and γd KCs (Fig. 4j).

Discussion

Our study describes a precise neural mechanism in *Drosophila* through which multisensory learning improves subsequent memory performance, even for individual sensory cues. We found that a single training trial with visual cues could only generate robust memory performance in flies if they were combined with odors during training, similar to visual rhythm perception learning in humans, which requires accompanying auditory information[47]. We show that multisensory learning binds together information from temporally contingent odors and colors within the axons of mushroom body γ KCs, via the serotonergic DPM neurons. Importantly, this learning-driven binding converts axons of visually (presumably color) selective KCs to also become responsive to the temporally contingent trained odor. While predominantly olfactory or visual dendritic input respectively defines γm KCs as being olfactory and γd as being visual, our recordings show that segments of their axons in the MB lobes become multimodal after multisensory learning. This result suggests that γ KCs are a likely substrate where other temporally contingent sensory information can be integrated with that of explicit sensory cues[48,49].

Although our experiments focused on odor activated γm KCs recruiting color γd KCs via DPM microcircuits, the observed behavioral enhancement of visual memory following multisensory learning and the connectivity of DPM neurons suggests that the reverse situation is also likely to apply. In so doing, multisensory learning links the KCs that are responsive to each temporally contingent sensory cue and expands the representation of each cue into that of the other. This cross-modal expansion allows the multisensory experience to be efficiently retrieved by the combined cues and by each individually. As a result, trained flies can evoke a memory of a visual experience with the learned odor, an effective form of synesthesia. These findings provide a neural mechanism through which the fly achieves a conceptual equivalent of hippocampus-dependent pattern completion in mammals, where partial cues are able to retrieve a more complete memory representation[50]. Interestingly, human patients with schizophrenia and autism exhibit deficits in multisensory integration[51,52] and these conditions have also been linked to serotonergic dysfunction and 5-HT2A receptor activity[53,54]. Our work

253 here suggests that inappropriate routing of multisensory percepts may contribute to these
254 conditions. Moreover, the excitatory 5-HT2A receptors that mediate multisensory binding, are
255 the major targets of hallucinogenic drugs[55].

Author contributions. Designed research Z.O., P.F.J., S.W., Performed research Z.O., P.F.J., C.S., K.D., N.O., P.V.G., Analyzed data Z.O., P.F.J, C.S., K.D., N.O., Resources S.W. Writing S.W., Z.O., P.F.J., N.O., Supervision S.W., Funding Acquisition S.W., Z.O.

Acknowledgments. We thank R. Brain, K. delos Santos, R. Busby, M. Moreno Gasulla, J-P. Moszynski and C. Talbot for technical assistance, G. Rubin, FlyLight, B. Dickson, A. Lin and the Vienna Drosophila Resource Center and the Bloomington Stock Center for flies. Z.O was funded by an EMBO Long-term postdoctoral fellowship (ALTF 311-2017). S.W. is funded by a Wellcome Principal Research Fellowship (200846/Z/16/Z), an ERC Advanced Grant (789274), and a Wellcome Collaborative Award (203261/Z/16/Z).

Online Content. Methods, along with additional Extended Data display items and Statistical Analysis, are available in the online version of the paper; references unique to these sections appear only in the online paper.

References

1. Stein, B. E., Stanford, T. R. & Rowland, B. A. Development of multisensory integration from the perspective of the individual neuron. *Nat. Rev. Neurosci.* **15**, 520–535 (2014).
2. Guo, J. & Guo, A. Crossmodal interactions between olfactory and visual learning. *Science.* **309**, 307–310 (2005).
3. Shams, L. & Seitz, A. R. Benefits of multisensory learning. *Trends Cogn. Sci.* **12**, 411–417 (2008).
4. Fetsch, C. R., Deangelis, G. C. & Angelaki, D. E. Bridging the gap between theories of sensory cue integration and the physiology of multisensory neurons. *Nat. Rev. Neurosci.* **14**, 429–442 (2013).
5. Vincis, R. & Fontanini, A. Associative learning changes cross-modal representations in the gustatory cortex. *Elife* **5**, 1–24 (2016).
6. Knöpfel, T. *et al.* Audio-visual experience strengthens multisensory assemblies in adult mouse visual cortex. *Nat. Commun.* **10**, (2019).
7. Han, X., Xu, J., Chang, S., Keniston, L. & Yu, L. Multisensory-Guided Associative Learning Enhances Multisensory Representation in Primary Auditory Cortex. *Cereb. Cortex* **32**, 1040–1054 (2022).
8. Aso, Y. *et al.* The neuronal architecture of the mushroom body provides a logic for associative learning. *Elife* **3**, e04577 (2014).
9. Li, F. *et al.* The connectome of the adult *Drosophila* mushroom body provides insights into function. *Elife* **9**, 1–217 (2020).
10. Owald, D. *et al.* Activity of Defined Mushroom Body Output Neurons Underlies Learned Olfactory Behavior in *Drosophila*. *Neuron* **86**, 417–427 (2015).
11. Cognigni, P., Felsenberg, J. & Waddell, S. Do the right thing: neural network mechanisms of memory formation, expression and update in *Drosophila*. *Curr. Opin. Neurobiol.* **49**, 51–58 (2018).
12. Tully, T. & Quinn, W. G. Classical conditioning and retention in normal and mutant *Drosophila melanogaster*. *J. Comp. Physiol. A.* **157**, 263–277 (1985).
13. Vogt, K. *et al.* Direct neural pathways convey distinct visual information to *Drosophila* mushroom bodies. *Elife* **5**, 1–13 (2016).
14. Schnaitmann, C., Pagni, M. & Reiff, D. F. Color vision in insects: insights from *Drosophila*. *J. Comp. Physiol. A Neuroethol. Sensory, Neural, Behav. Physiol.* **206**, 183–198 (2020).
15. Vogt, K. *et al.* Shared mushroom body circuits underlie visual and olfactory memories in *Drosophila*. *Elife* **3**, e02395 (2014).
16. Kitamoto, T. Conditional modification of behavior in *Drosophila* by targeted expression of a temperature-sensitive shibire allele in defined neurons. *J. Neurobiol.* **47**, 81–92

(2001).

17. Chamberland, S. *et al.* Fast two-photon imaging of subcellular voltage dynamics in neuronal tissue with genetically encoded indicators. *Elife* **6**, 1–35 (2017).
18. Burke, C. J. *et al.* Layered reward signalling through octopamine and dopamine in *Drosophila*. *Nature* **492**, 433–437 (2012).
19. Liu, C. *et al.* A subset of dopamine neurons signals reward for odour memory in *Drosophila*. *Nature* **488**, 512–516 (2012).
20. Lin, S. *et al.* Neural correlates of water reward in thirsty *Drosophila*. *Nat Neurosci* **17**, 1536–1542 (2014).
21. Schwaerzel, M. *et al.* Dopamine and octopamine differentiate between aversive and appetitive olfactory memories in *Drosophila*. *J. Neurosci.* **23**, 10495–502 (2003).
22. Riemensperger, T., Völler, T., Stock, P., Buchner, E. & Fiala, A. Punishment prediction by dopaminergic neurons in *Drosophila*. *Curr. Biol.* **15**, 1953–1960 (2005).
23. Claridge-Chang, A. *et al.* Writing Memories with Light-Addressable Reinforcement Circuitry. *Cell* **139**, 405–415 (2009).
24. Mao, Z. & Davis, R. L. Eight different types of dopaminergic neurons innervate the *Drosophila* mushroom body neuropil: Anatomical and physiological heterogeneity. *Front. Neural Circuits* **3**, 1–17 (2009).
25. Aso, Y. *et al.* Specific dopaminergic neurons for the formation of labile aversive memory. *Curr. Biol.* **20**, 1445–1451 (2010).
26. Aso, Y. *et al.* Three Dopamine Pathways Induce Aversive Odor Memories with Different Stability. *PLoS Genet.* **8**, e1002768 (2012).
27. Perisse, E. *et al.* Different Kenyon Cell Populations Drive Learned Approach and Avoidance in *Drosophila*. *Neuron* **79**, 945–956 (2013).
28. Krashes, M. J. *et al.* A Neural Circuit Mechanism Integrating Motivational State with Memory Expression in *Drosophila*. *Cell* **139**, 416–427 (2009).
29. Plaçais, P.-Y., Trannoy, S., Friedrich, A. B., Tanimoto, H. & Preat, T. Two Pairs of Mushroom Body Efferent Neurons Are Required for Appetitive Long-Term Memory Retrieval in *Drosophila*. *Cell Rep.* **5**, 769–780 (2013).
30. Plaçais, P. Y. & Preat, T. To favor survival under food shortage, the brain disables costly memory. *Science.* **339**, 440–442 (2013).
31. Waddell, S. Neural Plasticity : Dopamine Tunes the Mushroom Body Output Network. *Curr. Biol.* **26**, R109–R112 (2016).
32. Zheng, Z. *et al.* A Complete Electron Microscopy Volume of the Brain of Adult *Drosophila melanogaster*. *Cell* **174**, 1–14 (2018).
33. Clements, J. *et al.* neuPrint: Analysis Tools for EM Connectomics. *bioRxiv* (2020). doi:10.1101/2020.01.16.909465

34. Manoim, J. E., Davidson, A. M., Weiss, S., Hige, T. & Parnas, M. Lateral Axonal Modulation is Required for Stimulus-Specific Olfactory Conditioning in *Drosophila*. *bioRxiv* (2022). doi:10.1101/2022.06.02.494466

35. Waddell, S., Armstrong, J. D., Kitamoto, T., Kaiser, K. & Quinn, W. G. The amnesiac Gene Product Is Expressed in Two Neurons in the *Drosophila* Brain that Are Critical for Memory. *Cell* **103**, 805–813 (2000).

36. Yu, D., Keene, A. C., Srivatsan, A., Waddell, S. & Davis, R. L. *Drosophila* DPM neurons form a delayed and branch-specific memory trace after olfactory classical conditioning. *Cell* **123**, 945–957 (2005).

37. Pitman, J. L. *et al.* Report A Pair of Inhibitory Neurons Are Required to Sustain Labile Memory in the *Drosophila* Mushroom Body. *Curr. Biol.* **21**, 855–861 (2011).

38. Takemura, S. ya *et al.* A connectome of a learning and memory center in the adult *Drosophila* brain. *Elife* **6**, 1–43 (2017).

39. Liu, X. & Davis, R. L. The GABAergic anterior paired lateral neuron suppresses and is suppressed by olfactory learning. *Nat. Neurosci.* **12**, 53–59 (2009).

40. Zhou, M. *et al.* Suppression of GABAergic neurons through D2-like receptor secures efficient conditioning in *Drosophila* aversive olfactory learning. *Proc. Natl. Acad. Sci. U. S. A.* **116**, 5118–5125 (2019).

41. Aso, Y. *et al.* Nitric oxide acts as a cotransmitter in a subset of dopaminergic neurons to diversify memory dynamics. *Elife* **8**, 1–33 (2019).

42. Hearn, M. G. *et al.* A *Drosophila* dopamine 2-like receptor: Molecular characterization and identification of multiple alternatively spliced variants. *Proc. Natl. Acad. Sci. U. S. A.* **99**, 14554–14559 (2002).

43. Lark, A., Kitamoto, T. & Martin, J. R. Modulation of neuronal activity in the *Drosophila* mushroom body by DopEcR, a unique dual receptor for ecdysone and dopamine. *Biochim. Biophys. Acta - Mol. Cell Res.* **1864**, 1578–1588 (2017).

44. McGuire, S. E., Le, P. T., Osborn, A. J., Matsumoto, K. & Davis, R. L. Spatiotemporal Rescue of Memory Dysfunction in *Drosophila*. *Science.* **302**, 1765–1768 (2003).

45. Keene, A. C., Krashes, M. J., Leung, B., Bernard, J. A. & Waddell, S. *Drosophila* Dorsal Paired Medial Neurons Provide a General Mechanism for Memory Consolidation. *Curr. Biol.* **16**, 1524–1530 (2006).

46. Nichols, D. E. & Nichols, C. D. Serotonin receptors. *Chem. Rev.* **108**, 1614–1641 (2008).

47. Barakat, B., Seitz, A. R. & Shams, L. Visual rhythm perception improves through auditory but not visual training. *Curr. Biol.* **25**, R60–R61 (2015).

48. Jacob, P. F. *et al.* Prior experience conditionally inhibits the expression of new learning in *Drosophila*. *Curr. Biol.* **31**, 3490-3503.e3 (2021).

381 49. Zhao, B. *et al.* Long-term memory is formed immediately without the need for protein
382 synthesis-dependent consolidation in *Drosophila*. *Nat. Commun.* **10**, 4550 (2019).
383 50. Hunsaker, M. R. & Kesner, R. P. The operation of pattern separation and pattern
384 completion processes associated with different attributes or domains of memory.
385 *Neurosci. Biobehav. Rev.* **37**, 36–58 (2013).
386 51. Cascio, C. J., Simon, D. M., Bryant, L. K., DiCarlo, G. & Wallace, M. T.
387 *Neurodevelopmental and neuropsychiatric disorders affecting multisensory processes*.
388 *Multisensory Perception: From Laboratory to Clinic* (Elsevier Inc., 2019).
389 52. Siemann, J. K., Veenstra-VanderWeele, J. & Wallace, M. T. Approaches to
390 Understanding Multisensory Dysfunction in Autism Spectrum Disorder. *Autism Res.* **13**,
391 1430–1449 (2020).
392 53. Zhang, G. & Stackman, R. W. The role of serotonin 5-HT2A receptors in memory and
393 cognition. *Front. Pharmacol.* **6**, 1–17 (2015).
394 54. Muller, C. L., Anacker, A. M. J. & Veenstra-VanderWeele, J. The serotonin system in
395 autism spectrum disorder: From biomarker to animal models. *Neuroscience* **321**, 24–
396 41 (2016).
397 55. López-Giménez, J. F. & González-Maeso, J. Hallucinogens and Serotonin 5-HT2A
398 Receptor-Mediated Signaling Pathways. in *Brain Imaging in Behavioral Neuroscience*
399 45–73 (2017).
400 56. Hige, T. et al. Heterosynaptic Plasticity Underlies Aversive Olfactory Learning in
401 *Drosophila*. *Neuron* 88, 985–998 (2015).
402 57. Perisse, E. *et al.* Aversive Learning and Appetitive Motivation Toggle Feed-Forward
403 Inhibition in the *Drosophila* Mushroom Body. *Neuron* **90**, 1086–1099 (2016).
404

Methods

Fly strains. All *Drosophila melanogaster* strains were reared at 25 ˚C and 40-50% humidity, except where noted, on standard cornmeal-agar food (100 g l^{-1} anhydrous d-glucose, 47.27 g l^{-1} organic maize flour, 25 g l^{-1} autolyzed yeast, 7.18 g l^{-1} agar, 12.18 g Tegosept dissolved in 8.36 ml absolute ethanol, per liter of fly food) in 12:12 h light:dark cycle. Canton-S flies were used as wild-type (WT) and originated from William Quinn's laboratory (Massachusetts Institute of Technology, Cambridge, MA, USA). The following GAL4 lines were used in the behaviour experiments: MB607B-GAL4[1,2], c708a-GAL4[3], VT43924-GAL4.2[4], VT64246-GAL4[5]. Temperature controlled blocking of neuronal output was achieved by expressing the UAS-*Shi*^{ts1} [6] transgene under the control of the MB607B-GAL4[1,2], c708a-GAL4[3] and VT64246-GAL4[5] drivers. For RNA knockdown experiments, *tub*P-GAL80^{ts} [7], VT43924-GAL4.2[4] flies were crossed with UAS-Dop2R RNAi[8] and UAS-DopEcR RNAi (VDRC ID 103494) flies, and MB607B-GAL4[1,2] flies with UAS-5-HT2a RNAi (BDSC 31882), UAS-5-HT2b RNAi (BDSC 60488) and UAS-5-HT7 RNAi (BDSC 27273) flies. For live-imaging experiments UAS-ASAP2f[9] was expressed using the MB607B-GAL4[1,2] driver line. We used both male and female flies for behavior and imaging experiments.

Behavioral experiments. Male flies from the GAL4 lines were crossed to UAS-*Shi*^{ts1} virgin females, except for experiments involving c708a-GAL4, where UAS-*Shi*^{ts1} males were crossed to c708a-GAL4 virgin females. For heterozygous controls, GAL4 or UAS-*Shi*^{ts1} flies were crossed to WT flies. All flies were raised at 25 ˚C, except where noted below for manipulation of RNAi expression. Populations of 2–8 day-old flies were used in all experiments.

For appetitive conditioning experiments, 80-100 flies were placed in a 25 ml vial containing 1% agar (as a water source) and a 20 × 60 mm piece of filter paper for 19–22 h before training and were kept starved for the entire experiment, except when assaying 24 h memory where flies were fed for 30 min after training then returned to starvation vials until testing. For aversive conditioning experiments, 80-100 flies were placed in a vial containing standard food and a piece of filter paper for 14–22 h before behavioral experiments.

For experiments involving neuronal blocking with UAS-*Shi*^{ts1}, a schematic of the timing of the temperature shifting is provided in each figure. For *Shi*^{ts1} experiments, flies were transferred to restrictive 33 ˚C 30 min prior to training and/or testing. For RNAi experiments involving *tub*P-GAL80^{ts}; VT43924-GAL4.2, flies were raised at 18 ˚C and shifted to 29 ˚C after eclosion to induce RNAi expression for 3 d before the behavioral experiments. The flies remained at 29 ˚C for the duration of the experiments.

All behavioral experiments were conducted using a standard T-maze that was modified to allow simultaneous delivery of odor and color stimuli. The T-maze which is made from translucent plastic was covered in opaque blackout film to minimise interference between the visual stimuli when they were used in parallel. Odors were 4-methylcyclohexanol (MCH) and 3-octanol (OCT) diluted in mineral oil (at ≈1:10^{-3} dilution). Colors were provided by light-emitting diodes (LEDs); green LEDs with wavelength 425 +/- 10nm (ProLight Opto, PM2E-3LGE-SD) and blue LEDs with wavelength 465 +/- 10nm (ProLight Opto, PM2B-3LDE-SD). Four LEDs were assembled in a circuit built onto a heat sink and were mounted securely on top of the odor delivery tubes. The intensities of the LEDs were adjusted so that naïve flies showed no phototactic preference between the illuminated T-maze arms. Visual stimuli were presented in the same manner and same intensity for both training and testing. For appetitive experiments the testing tubes were lined with filter paper and for aversive experiments the testing tubes were lined with non-electrified shock grids. Experiments were performed in an environmental chamber set to the desired temperature and 55-65% relative humidity. Flies were handled prior to training and testing under overhead red light.

Appetitive conditioning was performed essentially as previously described[10]. Briefly, flies were exposed for 2 min to stimuli Y (Y_{Odor} and/or Y_{Color}) without reinforcement in a tube with dry filter paper (the Conditioned Stimulus minus, CS-), 30 s of clean air, then 2 min with stimuli X (X_{Odor} and/or X_{Color}) presented with 5.8 M sucrose dried on a filter paper (the Conditioned Stimulus plus, CS+). For aversive olfactory conditioning[11,12], flies recieved 1 min exposure to stimuli X (X_{Odor} and/or X_{Color}) paired with twelve 90 V electric shocks at 5 s intervals (CS+), 45 s of clean air, followed by 1 min exposure to stimuli Y (Y_{Odor} and/or Y_{Color}) without reinforcement (CS-). Electric shocks were delivered using a Grass S48 Square Pulse Stimulator (Grass Technology). Shock grids are those previously described[13] and consist of interleaved copper fingers printed on translucent Mylar film which allows color stimuli to penetrate.

Memory performance was assessed by testing flies for their preference between the CS- and the CS+ odors and/or colors for 2 min. Odor testing was performed in darkness. Performance Indices were calculated as the number of flies in the CS+ arm minus the number in the CS- arm, divided by the total number of flies. For all behavioral experiments, a single sample, or *n*, represents the average Performance Index from two independent groups of flies trained with the reciprocal odor/color combinations as CS+ and CS-.

Six behavioral protocols were used:

1) Visual Learning (V), colors (X_{Color} and Y_{Color}) were used as CS+ and CS-.

2) Olfactory Learning (O), odors (X_{Odor} and Y_{Odor}) were used as CS+ and CS-.
3) Congruent protocol (C), odors and colors were combined (X_{Color} + X_{Odor} and Y_{Color} + Y_{Odor}) as CS+ and CS-. The same odor + color combinations were used during training and testing.
4) Incongruent protocol (I) odor and color stimulus contingencies were switched between training (X_{Color} + Y_{Odor} and Y_{Color} + X_{Odor}) and testing (X_{Color} + X_{Odor} and Y_{Color} + Y_{Odor}).
The V and O protocols are unisensory, whereas C and I are multisensory.
5) Olfactory retrieval (OR), flies were trained as in the Congruent protocol (C), but only odors (X_{Odor} and Y_{Odor}) were presented as the choice at test.
6) Visual retrieval (VR), flies were trained as in the Congruent protocol (C), but only colors (X_{Color} and Y_{Color}) were presented as the choice at test.
The sequential learning experiments depicted in Figures 3k and 3l used aversive or appetitive Congruent multisensory training (C) followed by unisensory appetitive or aversive Olfactory learning (O) then testing using olfactory retrieval (OR).

Two-Photon Voltage Imaging. All flies were raised at 25 ˚C and 3–8 day-old male and female flies were used in all experiments. Imaging experiments were performed essentially as described previously[14–16]. In brief, flies were trained in the T-maze setup using either Olfactory learning (protocol 2 above), a Congruent multisensory protocol (3 above) or an Unpaired training protocol. In Unpaired training, flies were exposed to the combined odor and visual stimuli (X_{Odor}+X_{Color} and Y_{Odor}+Y_{Color} combination), but the shock or sugar was presented alone 2 min before or after the CS+, respectively. After training, flies were kept in darkness until recording. Just before recording, flies were briefly immobilized on ice and mounted in a custom-made chamber allowing free movement of the antennae and legs. The head capsule was opened under room temperature carbogenated (95% O2, 5% CO2) buffer solution and the fly, in the recording chamber, was placed under a Two-Photon microscope (Scientifica). For starved flies, the following sugar-free buffer was used: 108 mM NaCl, 5 mM KCl, 5 mM HEPES, 15 mM ribose, 4 mM $NaHCO_3$, 1mM NaH_2PO_4, 2 mM $CaCl_2$, 8.2 mM $MgCl_2$, osmolarity 272 mOsm, pH 7.3). For fed flies, the following buffer was used: 103 mM NaCl, 3 mM KCl, 5mM N-Tris, 10 mM trehalose, 10 mM glucose, 7mM sucrose, 26 mM $NaHCO_3$, 1mM NaH_2PO_4, 1.5 mM $CaCl_2$, 4mM $MgCl_2$, osmolarity 275 mOsm, pH 7.3).
Flies were subjected to a constant air stream, carrying vapor from mineral oil solvent (air). To emulate the testing phase, the flies were sequentially exposed to CS+ and CS- odor, each for 5 s, interspersed by 30 sec of air. As in the behavior experiments the odors were MCH and OCT (diluted in mineral oil at ≈1:10^{-3}), and they were used reciprocally as CS+ and CS-. One hemisphere of the brain was randomly selected to image the axons of KCs. Any flies that did not respond to one of the two presented odors were excluded from further analyses. Each *n* corresponds to a recording from a single fly.

Fluorescence was excited using ~140 fs pulses, 80 MHz repetition rate, centered on 910 nm generated by a Ti-Sapphire laser (Chameleon Ultra II, Coherent). Images of 256 x 256 pixels were acquired at 5.92 Hz, controlled by ScanImage 3.8 software[17]. Odors were delivered using a custom-designed system[18].

For acute 5-HT application, we used a perfusion pump system (Fisher Scientific US 14-284-201) to continuously deliver saline at a rate of ~0.043 mL/sec. 5-HT was applied in the presence of 1 µM tetrodotoxin (TTX) to block voltage-gated sodium channels and propagation of action potentials that could result in indirect excitation. To examine the effects of serotonin on γd KC membrane voltage, baseline fluorescence was recorded for 5 min before switching to a solution containing 100 µM serotonin hydrochloride (Sigma Aldrich, Cat# H9523) for an additional 5 min of recording. Washout was performed by changing the solution back to saline. The time of application and concentration of serotonin used is comparable to recent physiological studies applying exogenous serotonin to the *Drosophila* brain[19–22]. Due to perfusion tubing length and dead volume, the perfusion switch took approximately 70 s to reach the tissue.

For analysis, two-photon fluorescence images were manually segmented using Fiji[23], using a custom-made code including an image stabilizer plugin[24]. Movement of the animals was small enough such that images did not require registration. For subsequent quantitative analyses, custom Fiji and MATLAB scripts were used. The baseline fluorescence, F_0, was defined for each stimulus response as the mean fluorescence F from 2 s before and up to the point of odor presentation (or 30 s after the start of the recordings for 5-HT treatments). F/F_0 accordingly describes the fluorescence relative to this baseline. For the imaging of KCs, the area under the curve (AUC) was measured as the integral of $-\Delta F/F_0$ during the 5 s odor stimulation. The total number of flies, for each training protocol, came from 3 different training sessions.

For 5-HT treatments we defined the “pre-” treatment as the average $-\Delta F/F_0$ value for 300 s prior to the 5-HT delivery, the 5-HT application was the average $-\Delta F/F_0$ for 300 s during 5-HT delivery and the “washout-” treatment as the average $-\Delta F/F_0$ for 300 s from the offset of drug delivery. Traces were smoothed over 5 s by a moving average filter. The total number of flies were acquired from 3 different imaging sessions.

ASAP2f data are presented as $-\Delta F/F_0$ to correct the inverse relation between sensor fluorescence and membrane voltage.

Statistical Analysis. Statistical analyses were performed in GraphPad Prism. All behavioral data were analyzed with an unpaired t-test, Mann Whitney test or a one-way ANOVA followed by a posthoc Tukey's or Dunnet’s multiple comparisons test. No statistical methods were used

to predetermine sample size. For the imaging experiments odor-evoked responses were compared by a paired t-test for normally distributed data, otherwise a Wilcoxon matched-pairs signed rank test was used for non-Gaussian distributed data. Normality was tested using the D'Agostino & Pearson normality test. For imaging data, a method for outlier identification was run for each dataset (ROUT method), which is based on the False Discovery Rate (FDR). The FDR was set to the highest Q value possible (10%). In datasets in which potential outliers were identified, statistical analyses were performed by removing all odor-evoked responses for those flies. The analyses with or without the outliers were not different, so we decided to maintain and present the complete datasets, which may contain potential outliers.

Neuroanatomy, Connectivity, Dendrograms. Neuromorphological calculations and connectivity analyses were performed, and dendrograms calculated & plotted, using custom scripts based on NAVis 1.2.1 library functions in Python 3.8.8 (https://pypi.org/project/navis/; https://github.com/navis-org/navis)[25] and data from the *Drosophila* hemibrain (v.1.2.1) (https://neuprint.janelia.org)[26,27]. All neuronal skeletons were healed (navis.heal_skeleton (method = "ALL", max_dist = "100 nanometer", min_size = 10)), rerooted (navis.reroot_skeleton (x.soma)) and maximally down sampled with conserved connectors (navis.downsample_neuron(downsampling_factor = 1000, preserve_nodes = 'connectors')). 3D representations of neurons shaded by Strahler order were generated with navis.plot2d (method='3d', shade_by='strahler_index'), after pruning twigs with Strahler order ≤1 (navis.prune_by_strahler()). Where applicable only branches in specific volumes were considered (navis.in_volume()). Volumes were obtained from neuprint (v.1.2.1) with fetch_roi(). Connectivity was analyzed using unpruned neurons and with compartment specificity (navis.in_volume()).
Custom scripts based on navis.plot_flat() were used to generate dendrograms of DPM and APL neurons with twigs of Strahler order ≤1 pruned. MB compartment boundaries were defined by connectivity to DANs of the respective compartments. Branches outside the γ-lobe were downsized manually to increase visibility of γ-lobe compartments. Synapses are filtered by in_volume() and displayed on branches with Strahler order >1. Connectivity statistics are based on unpruned neurons and synapses between neurons were obtained with R based natverse:: neuprint_get_synapses (https://natverse.org)[25] scripts and processed with custom scripts in Python.

Data availability. Data supporting the findings of this study and customized MATLAB, Fiji R and python scripts are available from the corresponding author upon request.

References for Methods

1. Aso, Y. *et al.* Mushroom body output neurons encode valence and guide memory-based action selection in *Drosophila*. *Elife* **3**, e04580 (2014).
2. Aso, Y. *et al.* The neuronal architecture of the mushroom body provides a logic for associative learning. *Elife* **3**, e04577 (2014).
3. Zhu, S. *et al.* Gradients of the *Drosophila* Chinmo BTB-Zinc Finger Protein Govern Neuronal Temporal Identity. *Cell* **127**, 409–422 (2006).
4. Amin, H., Apostolopoulou, A. A., Suárez-Grimalt, R., Vrontou, E. & Lin, A. C. Localized inhibition in the *Drosophila* mushroom body. *Elife* **9**, 1–74 (2020).
5. Lee, P.-T. T. *et al.* Serotonin-mushroom body circuit modulating the formation of anesthesia-resistant memory in *Drosophila*. *Proc. Natl. Acad. Sci. U. S. A.* **108**, 13794–13799 (2011).
6. Kitamoto, T. Conditional modification of behavior in *Drosophila* by targeted expression of a temperature-sensitive shibire allele in defined neurons. *J. Neurobiol.* **47**, 81–92 (2001).
7. McGuire, S. E., Le, P. T., Osborn, A. J., Matsumoto, K. & Davis, R. L. Spatiotemporal Rescue of Memory Dysfunction in *Drosophila*. *Science.* **302**, 1765–1768 (2003).
8. Draper, I., Kurshan, P. T., McBride, E., Jackson, F. R. & Kopin, A. S. Locomotor activity is regulated by D2-like receptors in *Drosophila*: An anatomic and functional analysis. *Dev. Neurobiol.* **67**, 378–393 (2007).
9. Chamberland, S. *et al.* Fast two-photon imaging of subcellular voltage dynamics in neuronal tissue with genetically encoded indicators. *Elife* **6**, 1–35 (2017).
10. Krashes, M. J. & Waddell, S. Rapid Consolidation to a radish and Protein Synthesis-Dependent Long-Term Memory after Single-Session Appetitive Olfactory Conditioning in *Drosophila*. *J. Neurosci.* **28**, 3103–3113 (2008).
11. Tully, T. & Quinn, W. G. Classical conditioning and retention in normal and mutant *Drosophila melanogaster*. *J. Comp. Physiol. A.* **157**, 263–277 (1985).
12. Perisse, E. *et al.* Aversive Learning and Appetitive Motivation Toggle Feed-Forward Inhibition in the *Drosophila* Mushroom Body. *Neuron* **90**, 1086–1099 (2016).
13. Quinn, W. G., Harris, W. A. & Benzer, S. Conditioned behavior in *Drosophila melanogaster*. *Proc. Natl. Acad. Sci. U. S. A.* **71**, 708–12 (1974).
14. Owald, D. *et al.* Activity of Defined Mushroom Body Output Neurons Underlies Learned Olfactory Behavior in *Drosophila*. *Neuron* **86**, 417–427 (2015).
15. Felsenberg, J. *et al.* Integration of Parallel Opposing Memories Underlies Memory Extinction. *Cell* **175**, 709-722.e15 (2018).
16. Jacob, P. F. & Waddell, S. Spaced Training Forms Complementary Long-Term

627 Memories of Opposite Valence in *Drosophila*. *Neuron* **106**, 977-991.e4 (2020).
628 17. Pologruto, T. A., Sabatini, B. L. & Svoboda, K. ScanImage: Flexible software for
629 operating laser scanning microscopes. *Biomed. Eng. Online* **2**, 1–9 (2003).
630 18. Shang, Y., Claridge-Chang, A., Sjulson, L., Pypaert, M. & Miesenböck, G. Excitatory
631 Local Circuits and Their Implications for Olfactory Processing in the Fly Antennal Lobe.
632 *Cell* **128**, 601–612 (2007).
633 19. Zhang, X. & Gaudry, Q. Functional integration of a serotonergic neuron in the
634 *Drosophila* antennal lobe. *Elife* **5**, 1–24 (2016).
635 20. Liu, C. *et al.* A Serotonin-Modulated Circuit Controls Sleep Architecture to Regulate
636 Cognitive Function Independent of Total Sleep in *Drosophila*. *Curr. Biol.* **29**, 3635-
637 3646.e5 (2019).
638 21. Alekseyenko, O. V. *et al.* Serotonergic Modulation of Aggression in *Drosophila* Involves
639 GABAergic and Cholinergic Opposing Pathways. *Curr. Biol.* **29**, 2145-2156.e5 (2019).
640 22. Sampson, M. M. *et al. Serotonergic modulation of visual neurons in Drosophila*
641 *melanogaster*. *PLoS Genetics* **16**, (2020).
642 23. Schindelin, J. *et al.* Fiji: An open-source platform for biological-image analysis. *Nat.*
643 *Methods* **9**, 676–682 (2012).
644 24. Li, K. The image stabilizer plugin for ImageJ. (2008). Available at:
645 http://www.cs.cmu.edu/~kangli/code/Image_Stabilizer.html.
646 25. Bates, A. S. *et al.* The natverse, a versatile toolbox for combining and analysing
647 neuroanatomical data. *Elife* **9**, 1–35 (2020).
648 26. Scheffer, L. K. *et al.* A connectome and analysis of the adult *Drosophila* central brain.
649 *Elife* **9**, 1–74 (2020).
650 27. Clements, J. *et al.* neuPrint: Analysis Tools for EM Connectomics. *bioRxiv*
651 2020.01.16.909465 (2020).
652

Figure Legends

Figure 1. Multisensory learning enhances memory performance.

a. *Left*, Apparatus for multisensory training and testing. *Right*, training and testing timeline. **b.** Schematic of experimental protocols. Green and blue squares represent colors, light and dark grey squares represent 3-OCT and 4-MCH odors. Visual learning (V): colors were used as CS+ and CS-. Olfactory learning (O): odors were used as CS+ and CS-. Congruent protocol (C): pairs of colors and odors were combined as CS+ and CS-. Same color + odor combinations were used for training and testing. Incongruent protocol (I): colors and odors were combined as CS+ and CS- but color + odor combinations were switched between training and testing. Olfactory retrieval (OR): color and odor combinations were used for training but only odors for testing. Visual retrieval (VR): color and odor combinations were used for training but only colors for testing. **c** and **d.** *Top*, training and testing timelines. *Bottom*, immediate (**c**) and 6 h (**d**) memory performance for (V), (O), (C) and (I) protocols. Flies did not learn with colors alone (V). Performance was significantly increased when colors and odors were presented together. Congruent multisensory memory was significantly different than regular olfactory memory (O) and memory in the incongruent protocol (I) at all time points. At 6 h (**d**), memory performance for incongruent protocol (I) was significantly less than olfactory memory (O). **e** and **f.** *Top*, training and testing timelines. *Bottom*, multisensory training with colors + odors significantly enhanced immediate (**e**) and 6 h (**f**) memory for each individual modality. Performance retrieved with only odor (OR) or only colors (VR) was significantly greater than following unisensory olfactory (O) or visual learning (V). Asterisks denote significant differences ($P < 0.05$). Data presented as mean ± standard error of mean (SEM). Individual data points displayed as dots.

Figure 2. Enhanced performance following multisensory learning requires visually-responsive γd and $\alpha\beta_p$ Kenyon Cells.

a. *Top*, schematic of γd KCs. *Bottom*, training and testing timeline with temperature shifting (dashed line). *Right*, blocking output of γd KCs during testing using MB607B-GAL4; UAS-*Shi*^{ts1} impairs 6 h memory performance in the congruent protocol. **b**. Blocking γd KC output during testing improved 6 h memory performance in the incongruent protocol. **c.** *Top*, schematic of αβp KCs. *Bottom*, training and testing timeline with temperature shifting (dashed line). *Right*, blocking $\alpha\beta_p$ KC output during testing using c708a-GAL4; UAS-*Shi*^{ts1} reduces 6 h congruent memory performance. **d**. Blocking $\alpha\beta_p$ KC output during testing improved 6 h memory performance in the incongruent protocol. **e-f**. Blocking γd KC output during testing impaired Olfactory Retrieval of multisensory memory (**e**), whereas blocking $\alpha\beta_p$ KCs had no effect (**f**).

Asterisks denote significant difference ($P < 0.05$). Data presented as mean ± SEM. Individual data points displayed as dots. See Extended Data Fig. 2 for temperature controls.

Figure 3. γd Kenyon Cells become odor-activated after multisensory learning.

a. *Left*, appetitive multisensory (color + odor) training and imaging (odor) timeline. Imaging plane in the γ5 region of γd KC axons. *Middle*, traces of CS+ and CS- odor-evoked activity. The γ5 region of γd KC axons showed an excitatory response to the CS+ odor (a decrease in fluorescence increases the $-\Delta F/F_0$, of the ASAP2f voltage sensor). The same γ5 axons were inhibited by the CS- odor (decrease in $-\Delta F/F_0$). *Right*, quantification of odor-evoked responses. **b.** *Left*, appetitive multisensory (color+odor) training and imaging (odor) timeline. Imaging plane in the γ1 region of γd KC axons. *Middle*, traces of CS+ and CS- odor-evoked activity. Excitatory responses to CS+ odor were not observed in γ1 and the CS- odor elicited inhibition (decrease in $-\Delta F/F_0$). *Right*, quantification of odor-evoked responses. **c-d.** *Left*, appetitive unisensory (odor) training and imaging (odor) timelines. Imaging plane in the γ1 (**c**) and γ5 (**d**) regions of γd KCs. *Middle*, traces of CS+ and CS- odor-evoked activity. Both γ1 and γ5 regions show inhibition in response to CS+ and CS- odors (decrease in −ΔF/F0). *Right*, quantification of odor-evoked responses. For all traces and quantification, CS+ data correspond to average responses in which 50% of trials used MCH as CS+ and the others OCT was CS+. Same applies for CS- data. Odor-evoked activity traces show mean (solid line) with SEM (shadow). Black line underneath traces marks 5 s odor exposure. Asterisks denote significant difference between averaged CS+ and CS- responses ($P < 0.05$). CS+ and CS- responses for each individual fly are connected by a dashed line. **e.** MB model for appetitive multisensory color + odor training followed by unisensory odor testing. γ KCs project through the γ1- γ5 compartments of the horizontal γ lobe. γ main [γm] KCs receive olfactory input while γ dorsal [γd] are visually driven. Appetitive training (*left*) engages rewarding DANs (green) that innervate the γ4 and γ5 compartments. Dopamine encodes learning by directing depression of synapses between stimulus-activated KCs and avoidance-directing Mushroom Body Output Neurons (MBONs; not illustrated)[9]. Dopaminergic signalling during multisensory learning also binds γm and γd KC activity in the γ4-5 compartments. During subsequent unisensory testing (*right*) odor excites specific γm KCs (thick grey), which in turn activate γd axons in the γ4-5 compartments (grey dashed lines to yellow). The additional KC activity increases memory expression. **f.** MB model for aversive multisensory training followed by odor testing. Aversive multisensory training (*left*) engages punishment DANs (red) that depress synapses between γm and γd KCs and approach-directing MBONs[56,57] (not shown) in proximal γ1 and γ2 compartments, while also binding γd and γm KC activity in these compartments. Unisensory odor testing (*right*) excites specific γm KCs which also activates γd axons from γ1 forward. **g.**

Left, aversive multisensory training and odor imaging timeline. Imaging plane of γd KCs in the γ1 compartment. *Middle*, traces of CS+ and CS- odor-evoked activity. The γ1 region showed excitation to the CS+ and inhibition to the CS-. *Right*, quantification. **h.** *Left*, aversive multisensory training and odor imaging timeline. Imaging plane in the γ5 compartment of γd KCs. *Middle*, traces of CS+ and CS- odor-evoked activity. The CS+ odor evoked significantly less inhibition in this region than the CS-. *Right*, quantification. **i-j.** *Left*, aversive unisensory odor training and odor imaging timelines. Imaging plane in the γ1 (**c**) and γ5 (**d**) regions of γd KCs. *Middle*, traces of CS+ and CS- odor-evoked activity. Both γ1 and γ5 regions show inhibition in response to CS+ and CS- odors (decrease in −ΔF/F0). *Right*, quantification. **k**. Prior aversive multisensory learning enhances future appetitive odor learning. *Left*, protocols. Starved flies were divided into: Group I, aversive multisensory training, and Group II, unisensory odor training. 3 h later both groups were trained with odors and sugar reward (using the same CS+/CS- odors as for initial training) and tested immediately afterwards. *Right*, Group I, initially trained with the multisensory aversive protocol performed significantly better than Group II that were initially aversively trained with only odors. **l.** Prior appetitive multisensory learning does not improve future aversive odor learning. *Left*, starved flies were divided into: Group I, appetitive multisensory training, and Group II, unisensory odor training. 3 h later both groups received aversive odor training (same CS+/CS- as used for initial training) and were tested immediately. *Right*, Group I, initially trained with multisensory appetitive protocol, did not outperform Group II, initially trained with only odors.

Figure 4. DPM and APL neurons mediate multisensory stimulus binding.

a. *Left*, 3D representation of the MB (light grey) with Dorsal Paired Medial (DPM) neuron neurites of the γ lobes (teal). DPM trifurcates (asterisk) into dorsal (dark teal) and ventral branches (light teal) and a γ1 compartment branch. Neurites are shaded by Strahler order and twigs with Strahler order <1 are pruned. *Right*, detailed view of the γ lobe with γ1- γ5 compartment borders defined by dashed lines. DPM presynapses to γd KCs (yellow spheres) co-localize on the dorsal branch in the γ5 compartment. Input synapses from γm KCs (grey spheres) to DPM are located throughout the ventral and dorsal branches. In γ5, 450 of 585 γm KCs make synapses with the DPM neuron dorsal branch, where 89 of 98 γd KCs also receive DPM input. Anterior Paired Lateral (APL) neuron inputs (magenta spheres) localize along both DPM branches. **b**. A 2-dimensional dendrogram projection of DPM neurites (shades of teal – see Extended Data Figure 4 g for details). The γ1 compartment is marked and γ2-5 compartments are split between dorsal and ventral DPM neuron branches. Inputs from γm KCs (grey spheres) and outputs to γd KCs (yellow spheres) co-localize on compartment-specific branches. Inhibitory inputs from APL (magenta spheres) are distributed

763 across the DPM neurites. Detail of APL connectivity is shown in the Extended Data Figure 4
764 h. **c-d.** *Top*, Projection view of APL neuron. Training and testing timeline with temperature
765 shifting (dashed line). *Bottom*, Adult-restricted RNAi knockdown of Dop2R in APL neurons
766 using *tub*PGAL80^{ts};VT43924-GAL4.2 significantly impaired 6 h Olfactory Retrieval memory
767 performance after multisensory appetitive training (**c**), and reduced memory following
768 unisensory Olfactory learning (**d**). **e-f**. *Top*, Projection view of DPM neuron. Training and
769 testing timeline with temperature shifting (dashed line). *Bottom*, blocking DPM neuron output
770 with VT64246-GAL4; UAS-*Shi*^{ts1} during training (**e**) or testing (**f**) impaired 6 h Olfactory
771 Retrieval memory performance. See Extended Fig. 4e and f for controls. **g.** *Top*, training and
772 testing timeline. *Bottom*, RNAi knockdown of 5-HT2A, but not 5-HT2B or 5-HT7, receptors in
773 γd KCs with MB607B-GAL4 significantly impaired 6 h Olfactory Retrieval memory
774 performance. Data represented as mean ± SEM. Individual data points displayed as dots.
775 Asterisks denote significant difference ($P < 0.05$). **h-i.** *Left top*, imaging plane in the γ1 (**h**) and
776 γ5 (**i**) region of γd KCs. *Left bottom*, for all experiments, a baseline recording in saline (300 s;
777 not shown) was followed by perfusion with 100 μM serotonin (5-HT; 300 s) and by washout in
778 saline (300 s). Average traces for bath application and washout in γ1 (**h**) and γ5 (**i**) are shown.
779 *Right,* both regions show excitatory responses to 5-HT application (increased average –
780 $\Delta F/F_0$), in comparison to the baseline (pre) and after washout. All traces are a moving average
781 (solid line) with SEM (shadow). Asterisks denote significant difference between average signal
782 during 5-HT application compared to the pre and after conditions ($P < 0.05$). Values from each
783 individual fly are connected by dashed lines. **j.** Model of DPM microcircuit bridging of odor and
784 color specific KC streams following multisensory learning.
785

Extended Data Figure 1. Memory performance is most robust when color and odor combinations are consistent during acquisition and retrieval.

a. *Top left*, multisensory protocols. Green and blue squares represent colors, light and dark grey squares represent odors. Visual learning (V): colors used as CS+ and CS-. Olfactory learning (O): odors used as CS+ and CS-. Congruent protocol (C): pairs of colors and odors were combined as CS+ and CS-. Same color + odor combinations used during training and testing. Incongruent protocol (I): colors and odors were combined as CS+ and CS- but combinations were switched between training and testing. *Bottom left*, training and testing timeline. *Right*, 24 h memory performance for V, O, C and I protocols. Combining color and odor in the congruent protocol (C) enhanced 24 h performance, compared to that obtained with unisensory V or O learning. Incongruent (I) pairing of colors and odors abolished the multisensory enhancement of 24 h memory. **b.** *Left*, training and testing timeline. *Middle*, multisensory protocols. *Right*, immediate memory performance. Flies showed a significantly higher memory following the C than the I protocol. **c.** *Left*, training and testing timeline. *Middle*, multisensory protocols: C protocol as above. Odors were each paired with a different color as CS+ and CS-; odor + color combinations were identical at training and testing. Congruent protocol using the same color (C-sc) combined with different odors as CS+ and CS- during training and testing. *Right*, the C protocol using distinct color and odor combinations for CS+ vs CS- resulted in higher immediate memory performance than the C-sc protocol using the same color with both odors. **d.** *Left*, training and testing timeline. *Middle,* multisensory protocols: Olfactory learning (O) as above: odors were used as CS+ and CS- during training and testing. *(2)* Multisensory Retrieval (MSR): odors were CS+ and CS- during training and these same odors were combined with different colors during testing. *Right*, immediate memory performance evoked by MSR was not significantly reduced to that following for Olfactory learning and retrieval. **e.** *Left*, training and testing timeline. *Middle,* multisensory protocols: Congruent (C) protocol as above: different colors and odors were combined as CS+ and CS- during training and testing. Odor retrieval (OR): colors + odors were CS+ and CS- during training and only odors were used during testing. *Right*, flies trained with multisensory stimuli performed better if they were tested with congruent multisensory stimuli compared to only one modality (in this case odor). Data presented as mean ± SEM. Individual data points displayed as dots. Asterisks denote significant difference ($P < 0.05$).

Extended Data Figure 2. Constitutively blocking γd or $\alpha\beta_p$ KC output impairs the visual component of multisensory memories.

a. *Top left*, schematic of γd KCs. *Bottom left*, training and testing timeline with constant restrictive temperature (dashed line). *Right*, 6 h memory performance following odor learning is unchanged when γd KCs are blocked through the experiment using MB607B-GAL4; UAS-

Shi^{ts1}. **b** and **c.** Blocking γd KCs throughout the experiment significantly impaired memory in the Congruent protocol (**b**). The release from the interference effect of the Incongruent protocol did not reach significance (**c**). **d.** *Top left*, schematic of $\alpha\beta_p$ KCs. *Bottom left*, training and testing timeline with constant restrictive temperature (dashed line). *Right*, blocking /β_p KC output throughout the experiment using c708a-GAL4; UAS-*Shi*^{ts1} did not impair 6 h odor memory. **e-f.** Memory performance for Congruent (**e**) and Incongruent (**f**) protocols changed significantly when $\alpha\beta_p$ KCs were blocked during the experiment. **g** and **h**. *Top*, training and testing timeline with temperature shifting (dashed line). Blocking γd (**g**) and αβp (**h**) KCs impaired memory retrieved with Visual cues. **i.** *Top left*, schematic of γd KCs. *Top right*, training and testing timeline with constant permissive temperature (dashed line). **i-l** Memory performance in MB607B-GAL4; UAS-*Shi*^{ts1} flies following Congruent (**i**), Incongruent (**j**), Olfactory retrieval (**k**) and Visual retrieval (**l**) protocols was not affected when training and testing was performed at 23 ˚C. **m.** *Top left*, schematic of αβp KCs. *Top right*, training and testing timeline with constant permissive temperature (dashed line). **m-o** Memory performance in c708a-GAL4; UAS-*Shi*^{ts1} flies after Congruent (**m**), Incongruent (**n**), and Visual retrieval (**o**) protocols was not affected when training and testing was at 23 ˚C. Data presented as mean ± SEM. Individual data points displayed as dots. Asterisks denote significant difference ($P < 0.05$).

Extended Data Figure 3. Multisensory aversive learning enhances memory for the combined and individual odor and color cues.

a and **b.** Unpaired multisensory appetitive training does not alter γd KC odor responses.*Top left*, unpaired appetitive training and odor imaging protocol. Odor + color presentation was not contingent with sugar. *Bottom left*, imaging plane in the γ5 region (**a**) and γ1 (**b**) of γd KCs. *Middle*, traces of CS+ and CS- odor-evoked activity. In both regions the γd KCs were inhibited by CS+ and CS- odor presentation (increase in fluorescence = decrease in $-\Delta F/F_0$, of ASAP2f sensor). *Right*, CS+ and CS- odor-evoked responses showed a marked decrease in $-\Delta F/F_0$ and were not significantly different between each other. **c-h.** Multisensory aversive learning enhances memory for the combined and individual odor and color cues. **c.** *Top*, multi- and unisensory aversive training and testing protocols. *Bottom*, multisensory experiment conditions. Green and blue squares represent colors, light and dark grey represent odors. Visual learning (V); Olfactory learning (O); Congruent protocol (C); Incongruent protocol (I); Olfactory Retrieval (OR); Visual retrieval (VR). **d-f.** *Top*, training and testing timelines. *Bottom*, aversive memory with C protocol was significantly increased to that with I protocol at both immediately (**d**) and 3 h (**e**) after training. Flies in the C protocol outperformed those tested 3 h after Olfactory Learning (O). Only the C protocol generated significant 24 h memory performance (**f**). **g** and **h.** *Top*, training and testing timelines. When tested immediately (**g**),

multisensory memory retrieved with colors (VR) was markedly better than that following unisensory Visual learning (V). At 3 h multisensory trained flies performed significantly better when their memory was retrieved with only visual (VR) or olfactory (OR) cues than flies trained with unisensory odor (O) or visual (V) learnin. Data presented as mean ± standard error of mean (SEM). Individual data points displayed as dots. Asterisks denote significant differences ($P < 0.05$). **i** and **j.** Unpaired multisensory aversive training does not alter γd KC odor responses. *Left*, unpaired aversive multisensory training protocol and odor imaging protocol. Odor + color presentation was not contingent with shock. Imaging plane in the γ1 region (**i**) and γ5 region (**j**) of γd KCs. *Middle*, traces of CS+ and CS- odor-evoked activity. γd KCs were inhibited by the presentation of both odors. *Right*, quantification.

Extended Data Figure 4. DPM and APL neurons mediate multisensory stimulus binding. **a-b.** *Top*, training and testing timeline with temperature (dashed line). *Bottom*, 6 h Olfactory Retrieval of appetitive multisensory memory (**a**) and of memory following Olfactory learning (**b**) was not affected by RNAi knockdown of DopEcR in APL neurons using *tub*PGAL80^{ts}; VT43924-GAL4.2. **c-d**. Permissive 23 ˚C control experiment for Figure 4c (**c**) and 4d (**d**). *Top*, training and testing timeline with temperature shift (dashed line). Memory performance was unaffected in *tub*PGAL80^{ts};VT43924-GAL4.2, UAS-Dop2R RNAi flies following Olfactory retrieval (**c**) and Olfactory learning (**d**) when trained and tested at 23˚C. **e**. *Top*, training and testing timeline with temperature shifting (dashed line). *Bottom*, Blocking output from DPM neuron during training and testing with VT64246-GAL4; UAS-*Shi*^{ts1} did not impact memory after Olfactory learning. **f.** Permissive 23˚C control experiment for Figure 4e and f. Multisensory memory performance evoked by Olfactory retrieval of VT64246-GAL4; UAS-*Shi*^{ts1} flies was unaffected when trained and tested at 23 ˚C. Data presented as mean ± SEM. Individual data points displayed as dots. **g.** A 2-dimensional dendrogram projection of DPM neuron neurites (shades of teal). The dorsal branch of the horizontal lobe's γ2-γ5 compartments are dark teal, the rest of the γ lobe is medium teal and projections in the other lobes are light teal. Note: all but γ lobe neurites are downsized for visibility. Neurites with Strahler order <1 are pruned and connectivity is shown accordingly. The γ1 compartment is marked and γ2-5 compartments are split between dorsal and ventral DPM neuron branches, according to their DAN connectivity (shaded areas). Synapses (spheres) are only marked in the γ lobe compartments. The connectivity structure shows inputs from γd KCs (yellow spheres) and outputs to γm KCs (grey spheres) colocalize on compartment specific branches of the DPM neurons. APL inputs (magenta) are distributed across both dorsal and ventral branches and concentrated around the branching point at the base of the vertical lobes in the α'1 compartment (asterisk). Note: Some putative parts of the dorsal γ lobe branch could not be allocated to a compartment due to lack of DAN input. One branch that bears γ KC synapses

(hashtag) was identified as the β' lobe branch that enters the MB close to the midline. It is likely that other DPM neurite tips that have γ KC synapses are artifacts where healing has merged free-floating γ lobe branchlets to DPM neurites innervating the other lobes. **h:** A 2-dimensional dendrogram projection of APL neuron neurites (magenta). Note: Neurites with Strahler order <1 were pruned and connectivity is shown accordingly. Compare with (**g**). PPL1-γ1pedc and PAM-γ5 DAN input synapses (red and green spheres respectively) are marked in the γ1 and γ5 compartments (shaded areas). Synapses to DPM (teal spheres) colocalize with DAN input.

Figure 1

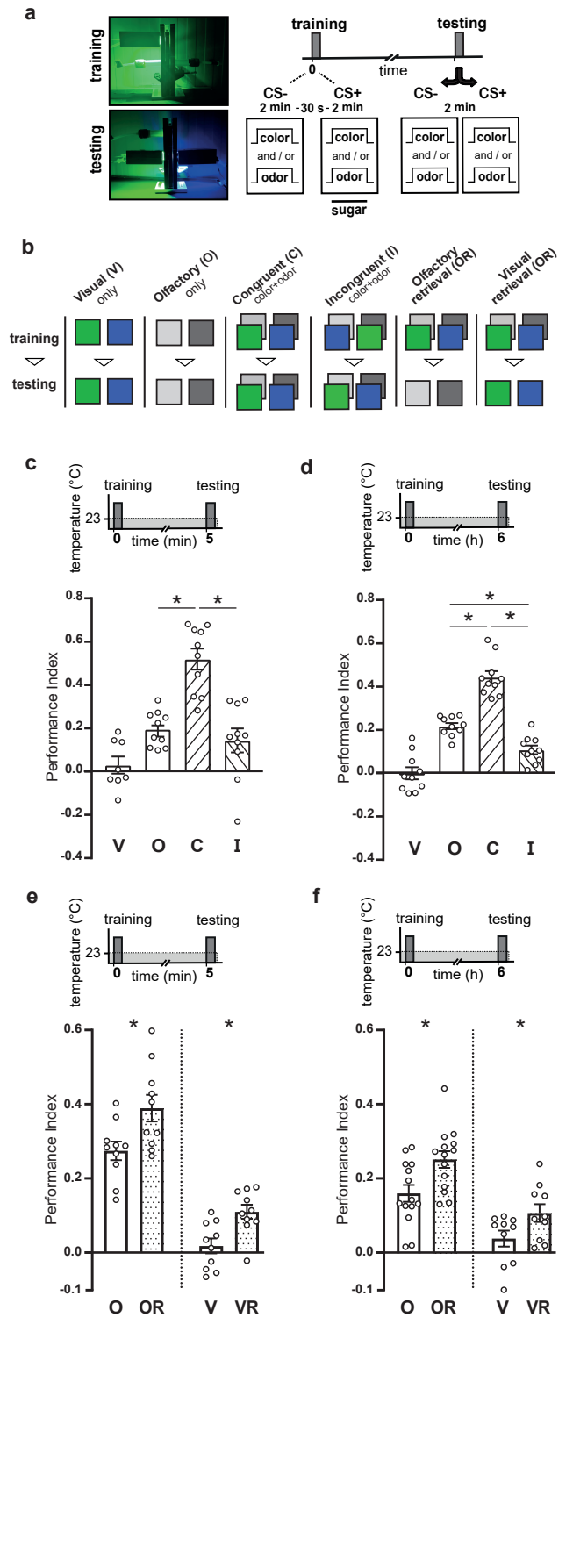
a
training
testing
training
testing
0
time
CS-
CS+
2 min -30 s- 2 min
CS-
CS+
2 min
color
and / or
odor
sugar
b
Visual (V) only
Olfactory (O) only
Congruent (C) color+odor
Incongruent (I) color+odor
Olfactory retrieval (OR)
Visual retrieval (OR)
training
testing
c
temperature (°C)
23
training
testing
0
time (min)
5
Performance Index
0.8
0.6
0.4
0.2
0.0
-0.2
-0.4
V
O
C
I
d
temperature (°C)
23
training
testing
0
time (h)
6
Performance Index
V
O
C
I
e
temperature (°C)
23
training
testing
0
time (min)
5
Performance Index
0.6
0.4
0.2
0.0
-0.1
O
OR
V
VR
f
temperature (°C)
23
training
testing
0
time (h)
6
Performance Index
O
OR
V
VR

Figure 2

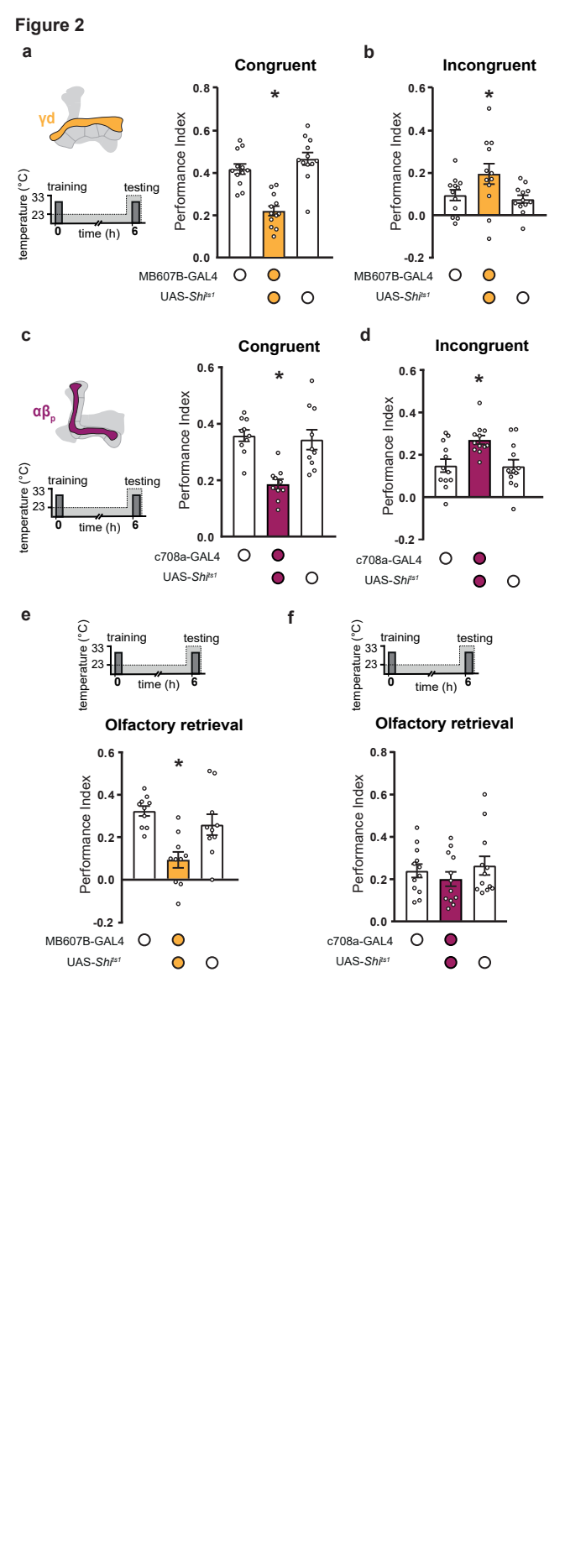
a
γd
training
testing
temperature (°C)
33
23
0
time (h)
6
Congruent
Performance Index
0.8
0.6
0.4
0.2
0.0
*
MB607B-GAL4
UAS-Shits1
b
Incongruent
Performance Index
0.6
0.4
0.2
0.0
-0.2
*
MB607B-GAL4
UAS-Shits1
c
αβp
training
testing
temperature (°C)
33
23
0
time (h)
6
Congruent
Performance Index
0.6
0.4
0.2
0.0
*
c708a-GAL4
UAS-Shits1
d
Incongruent
Performance Index
0.6
0.4
0.2
0.0
-0.2
*
c708a-GAL4
UAS-Shits1
e
training
testing
temperature (°C)
33
23
0
time (h)
6
Olfactory retrieval
Performance Index
0.6
0.4
0.2
0.0
-0.2
*
MB607B-GAL4
UAS-Shits1
f
training
testing
temperature (°C)
33
23
0
time (h)
6
Olfactory retrieval
Performance Index
0.8
0.6
0.4
0.2
0.0
c708a-GAL4
UAS-Shits1

Figure 3

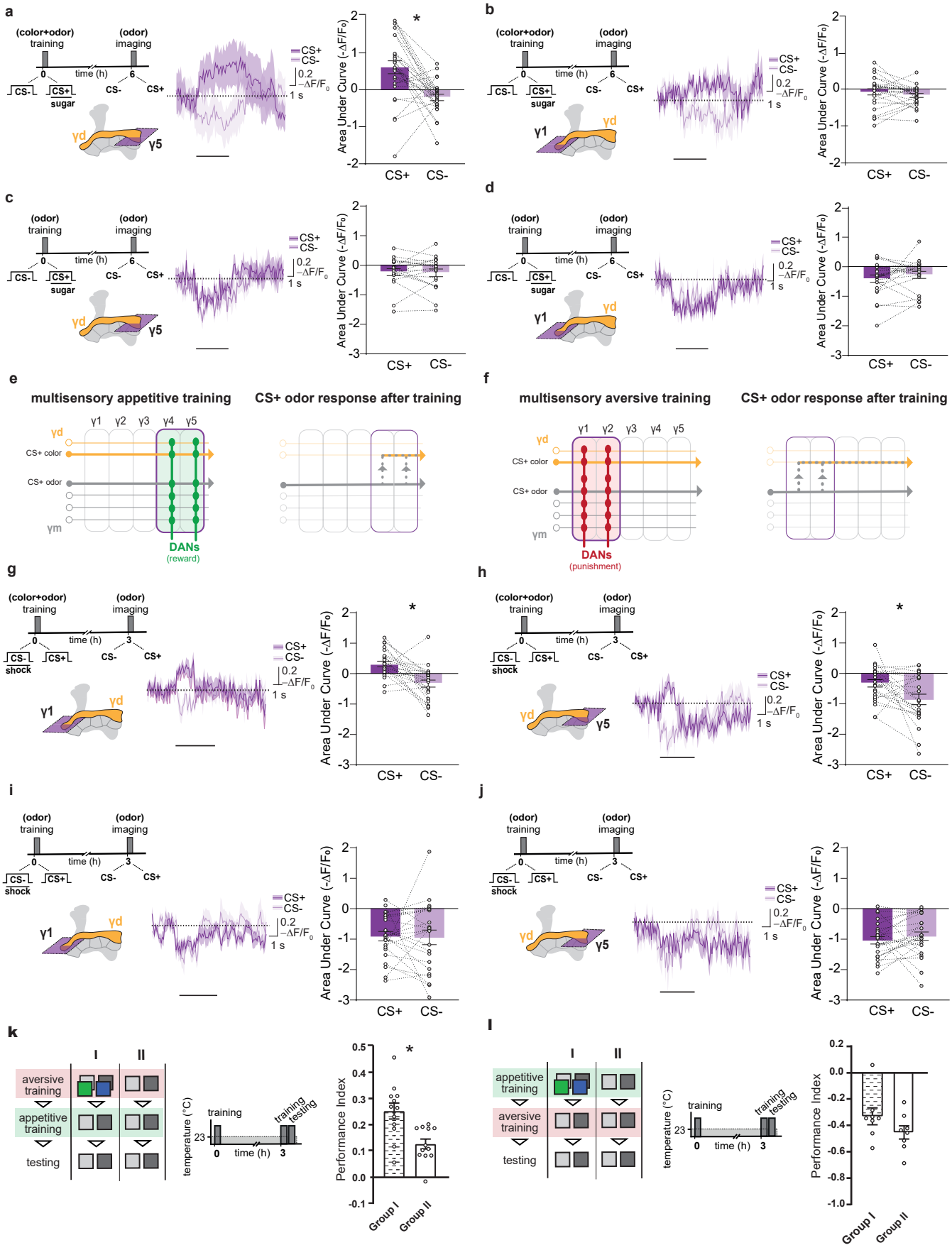
a
(color+odor) training
(odor) imaging
time (h)
CS-
CS+ sugar
CS-
CS+
γd
γ5
CS+
CS-
0.2 −ΔF/F0
1 s
Area Under Curve (-ΔF/F0)
CS+
CS-
b
γ1
γd
c
d
e
multisensory appetitive training
CS+ odor response after training
γ1 γ2 γ3 γ4 γ5
γd
CS+ color
CS+ odor
γm
DANs
(reward)
f
multisensory aversive training
CS+ odor response after training
DANs
(punishment)
g
(odor) training
(odor) imaging
CS- shock
h
i
j
k
aversive training
appetitive training
testing
I
II
temperature (°C)
training
training testing
Performance Index
Group I
Group II
l

Figure 4